Supporting Information

A Cost-Effective Dual-Anion Electrolyte Stabilizing Silicon Anodes via a Conductive LiF-Li_2O-LiCl-Rich Interphase

Tianyang Hong [a], Di Liu [a], Zhengguang Song [b], Xianting Zhao [a], Chenduan Xie [a], Xiaoqin Yi [a], Junxiong Wu [b], Yuming Chen [b], Xianhui Zhang [a, *]

a. Strait Institute of Flexible Electronics (SIFE, Future Technologies), Fujian Key Laboratory of Flexible Electronics and Strait Laboratory of Flexible Electronics (SLoFE), Fujian Normal University, Fuzhou, 350117, Fujian, China

b. Engineering Research Center of Polymer Green Recycling of Ministry of Education, Fujian Key Laboratory of Pollution Control & Resource Reuse, College of Environmental and Resource Sciences and College of Carbon Neutral Modern Industry, Fujian Normal University, Fuzhou, 350117, Fujian, China

*Corresponding author:

Xianhui Zhang

Email: [ifexhzhang@fjnu.edu.cn]

Address: College of Strait Flexible Electronics (Future Technology), Fujian Normal University, Fuzhou 350117, Fujian, China

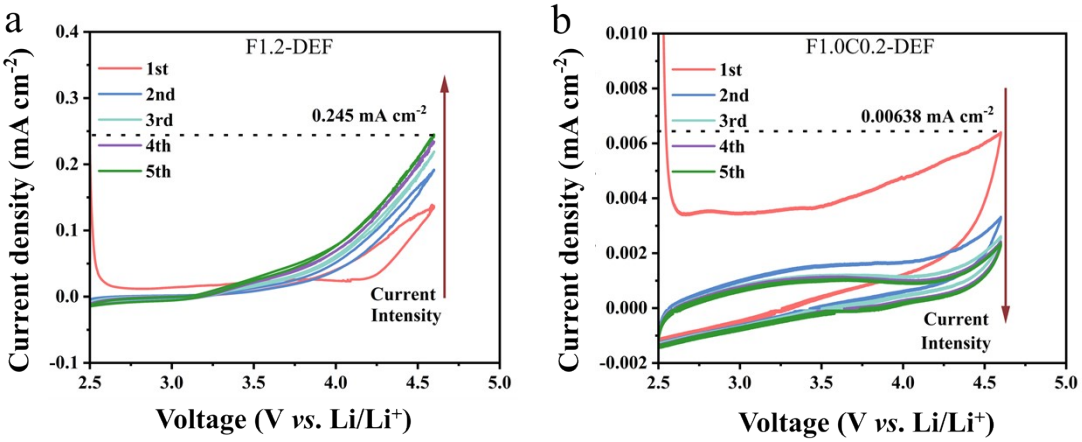

Fig. S1. CV curves of Li||Al cells measured between 2.5 and 4.6 V at a scan rate of 1 mV s^{-1}: (a) F1.2-DEF; (b) F1.0C0.2-DEF.

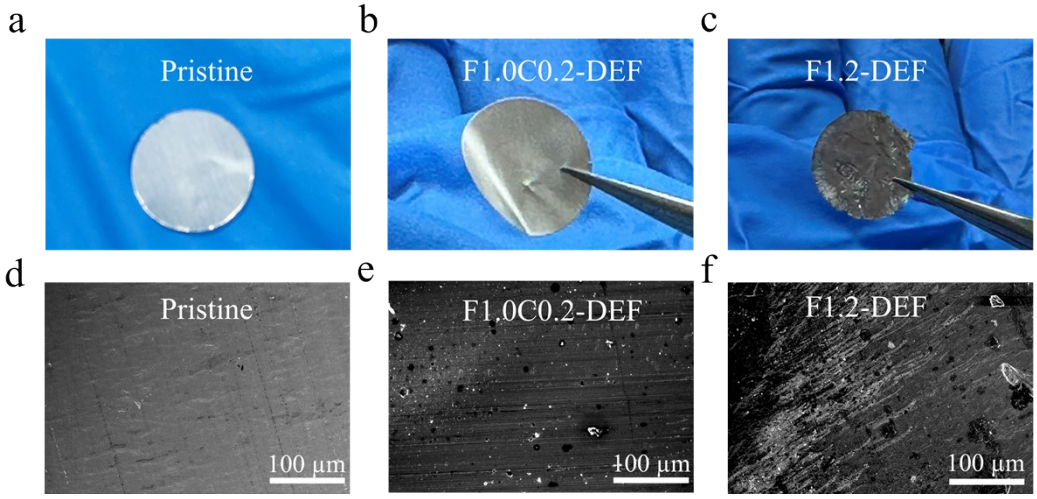

Fig. S2. Corrosion behavior of aluminum (Al) current collectors under electrochemical cycling: (a-c) Optical images of (a) pristine Al current collector (control) and (b, c) Al collectors after 5 CV cycles (2.5 – 4.6 V) in (b) F1.0C0.2-DEF and (c) F1.2-DEF; (d-f) SEM images of (d) pristine Al (uncycled) and (e, f) Al collectors after 5 CV cycles in (e) F1.0C0.2-DEF and (f) F1.2-DEF.

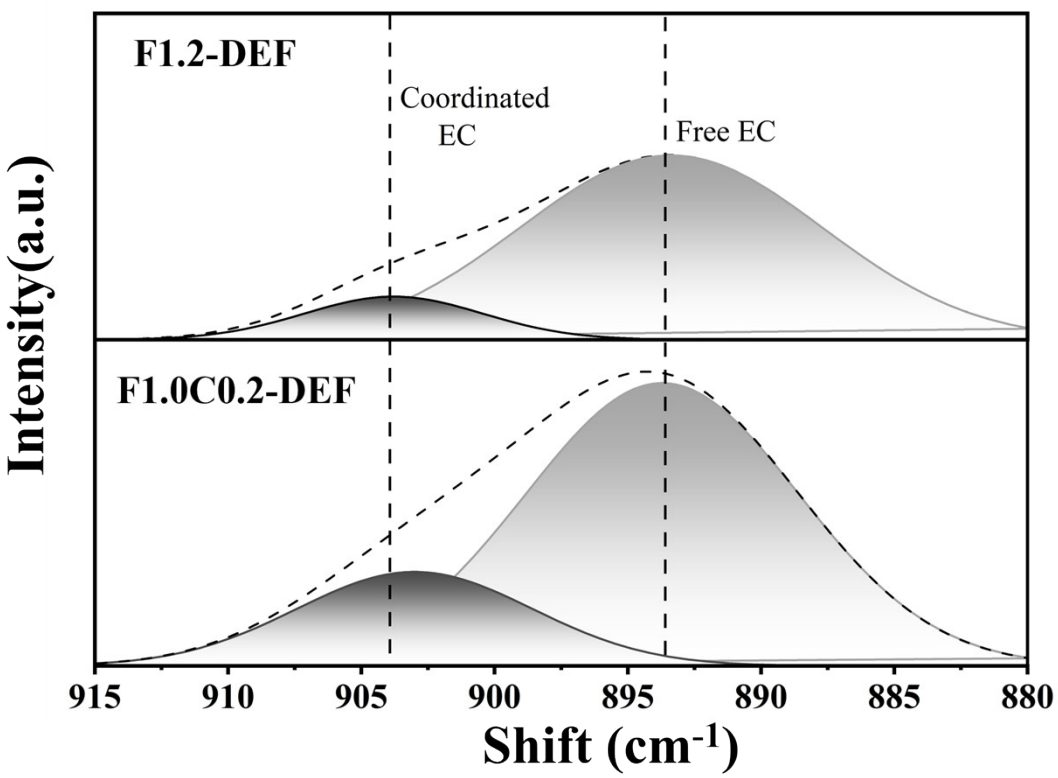

Fig. S3. Raman spectra in a wavenumber range from 880 to 915 cm^{-1}.

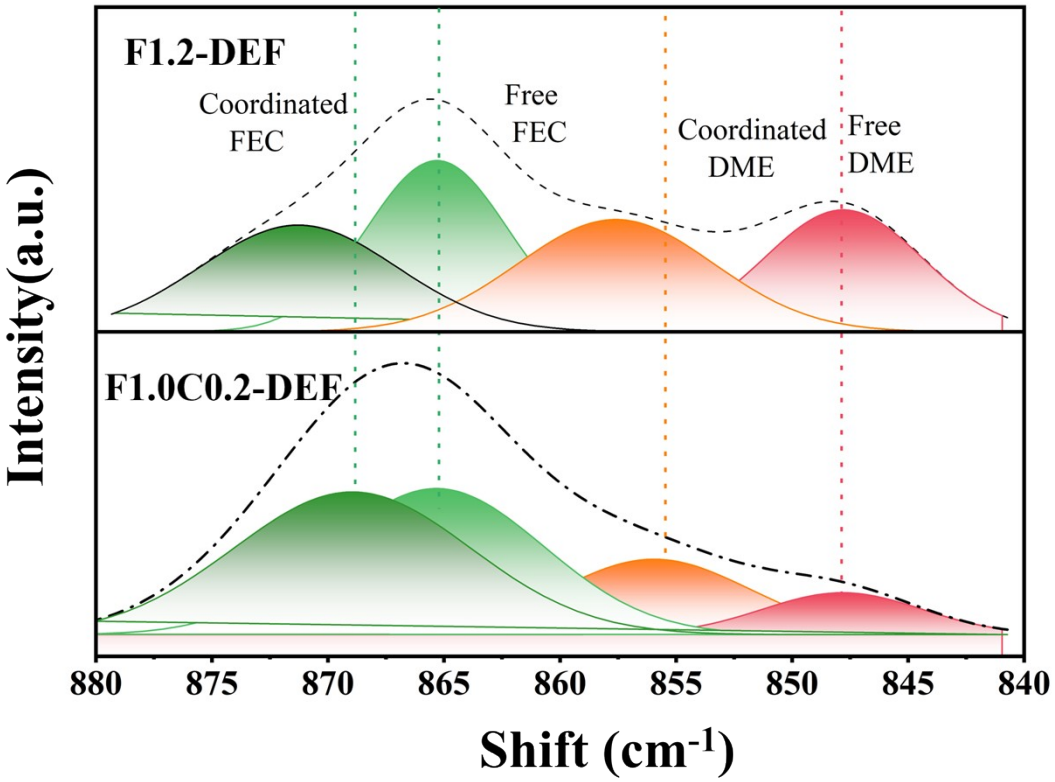

Fig. S4. Raman spectra in a wavenumber range from 840 to 880 cm^{-1}.

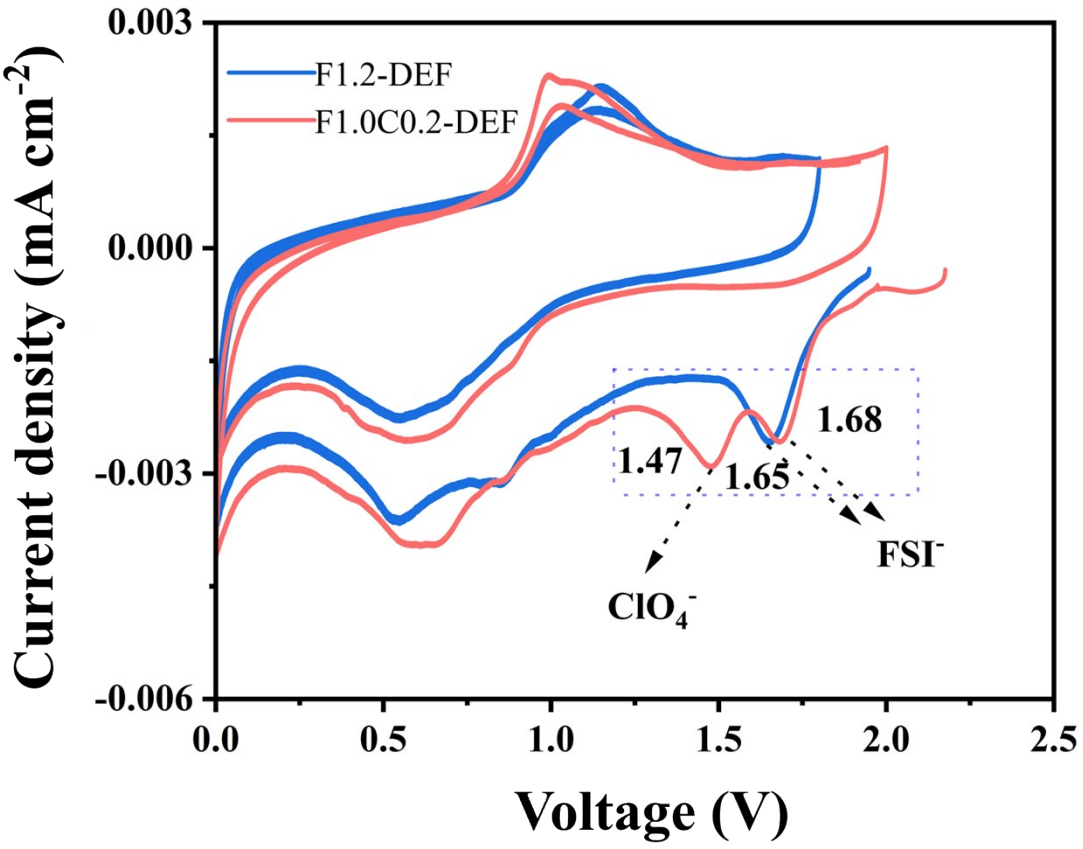

Fig. S5. CV curves of Li||Cu cells in the two studied electrolytes with the first scan conducted from the open circuit potential (OCP) to 0 V *vs*. Li/Li^+.

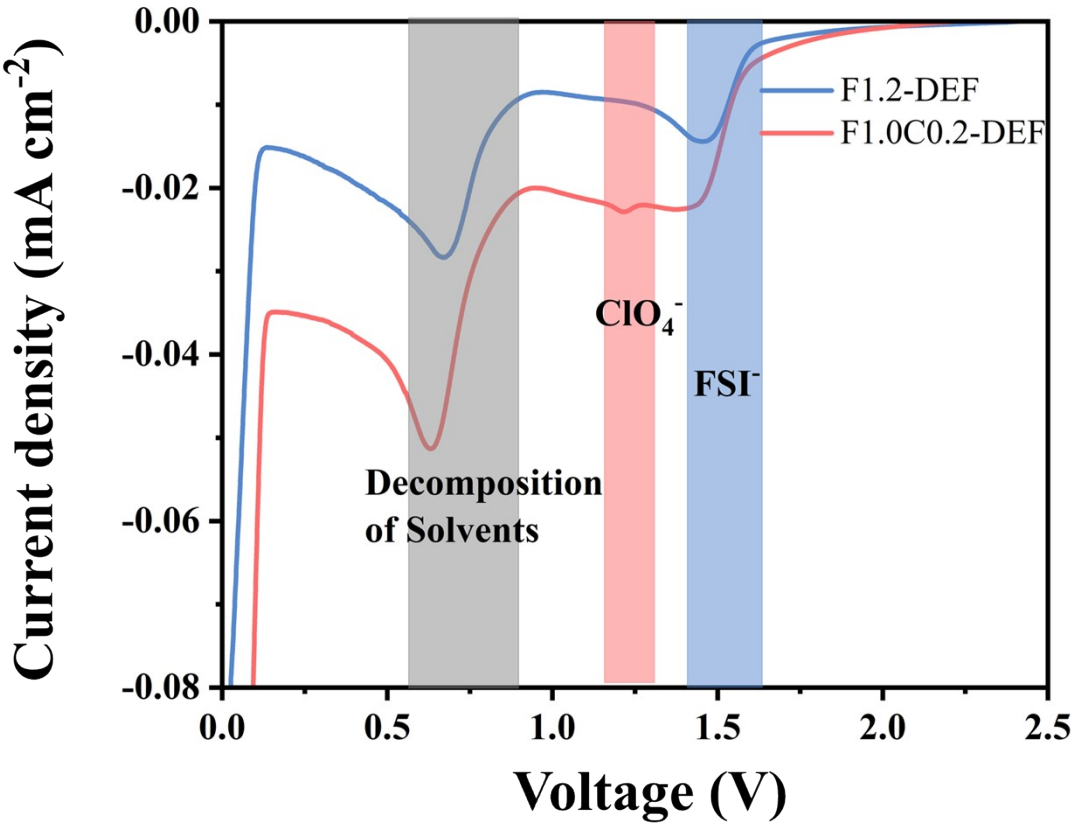

Fig. S6. LSV curves of Li||Al cells at a scan rate of 0.5 mV s^{-1} in F1.2-DEF and F1.0C0.2-DEF electrolytes.

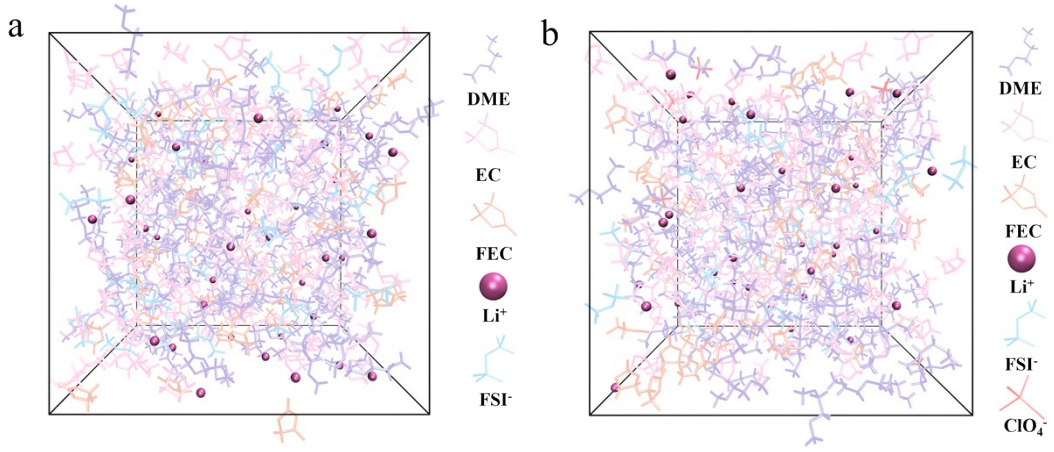

Fig. S7. Molecular dynamics (MD) simulation snapshots of electrolyte solvation structures: (a) F1.2-DEF (1.2 M lithium bis(fluorosulfonyl)imide (LiFSI) in dimethoxyethane (DME) / ethylene carbonate (EC) / fluoroethylene carbonate (FEC)) and (b) F1.0C0.2-DEF (1.0 M LiFSI + 0.2 M lithium perchlorate ($LiClO_4$) in DME/EC/FEC (10:7:3, *v/v/v*)).

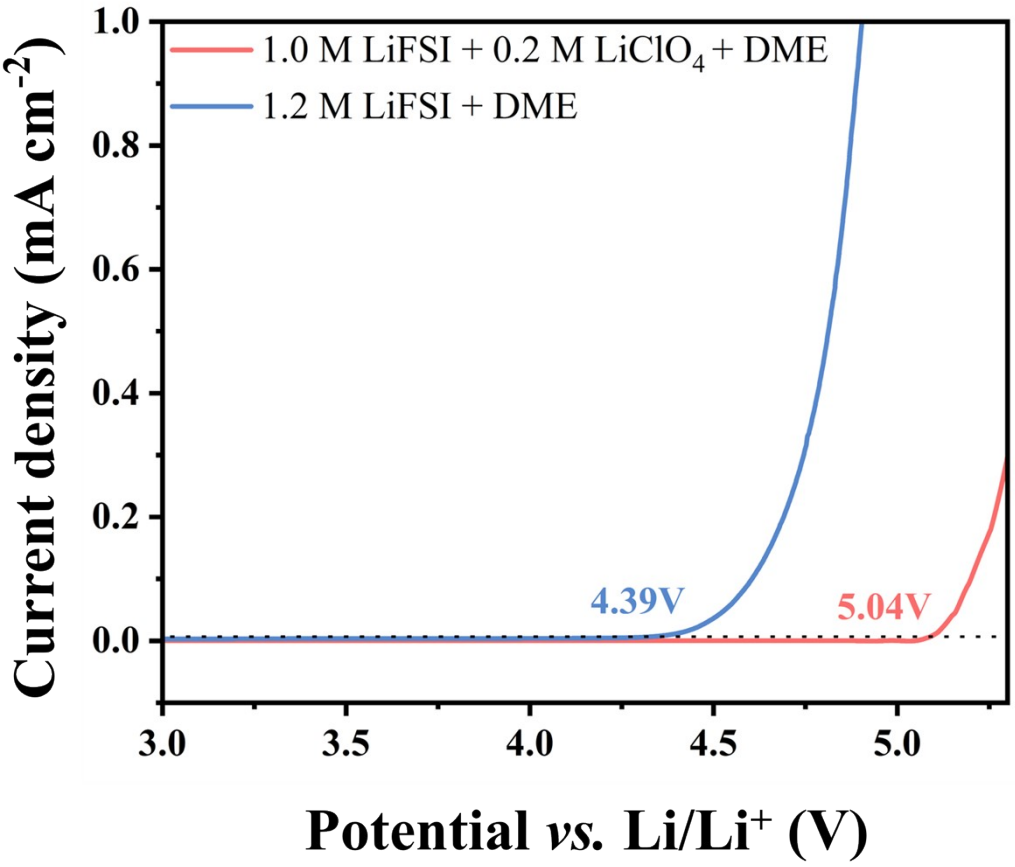

Fig. S8. LSV curves of Li||Al cells at a scan rate of 1 mV s^{-1} in different electrolytes.

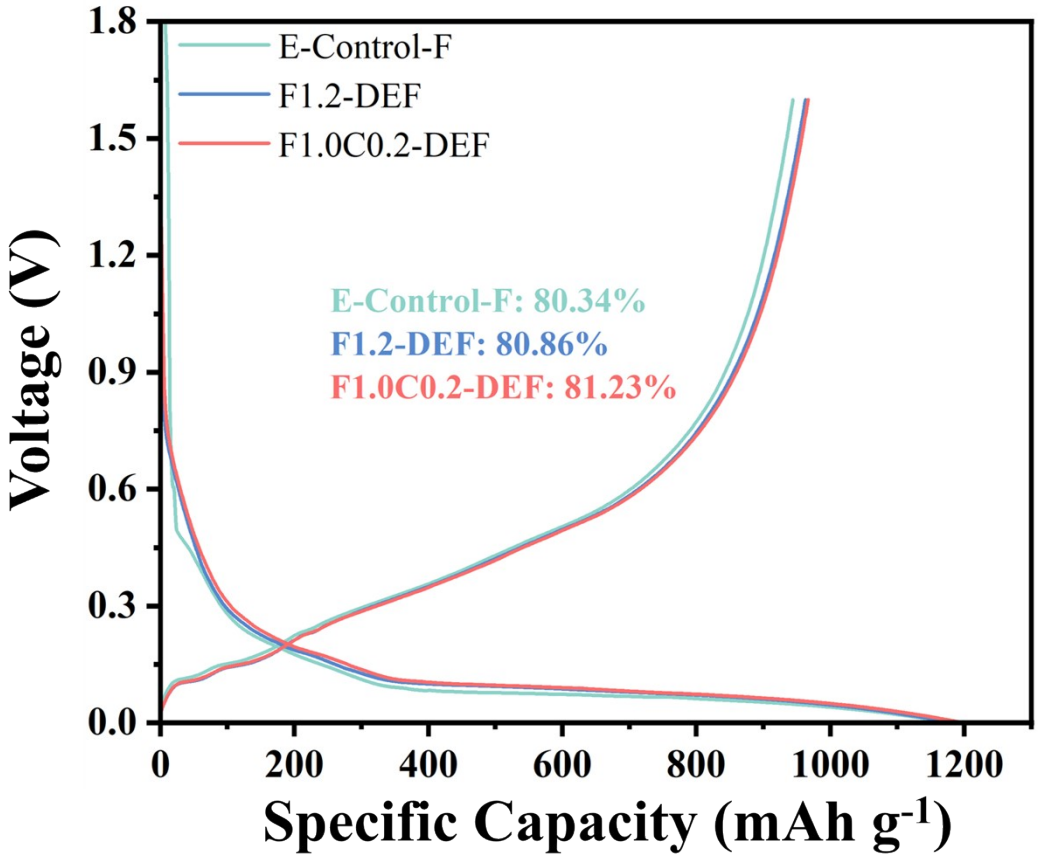

Fig. S9. Initial discharge/charge profiles of Li||Si/C cells in different electrolytes at 0.05C rate under 25 °C.

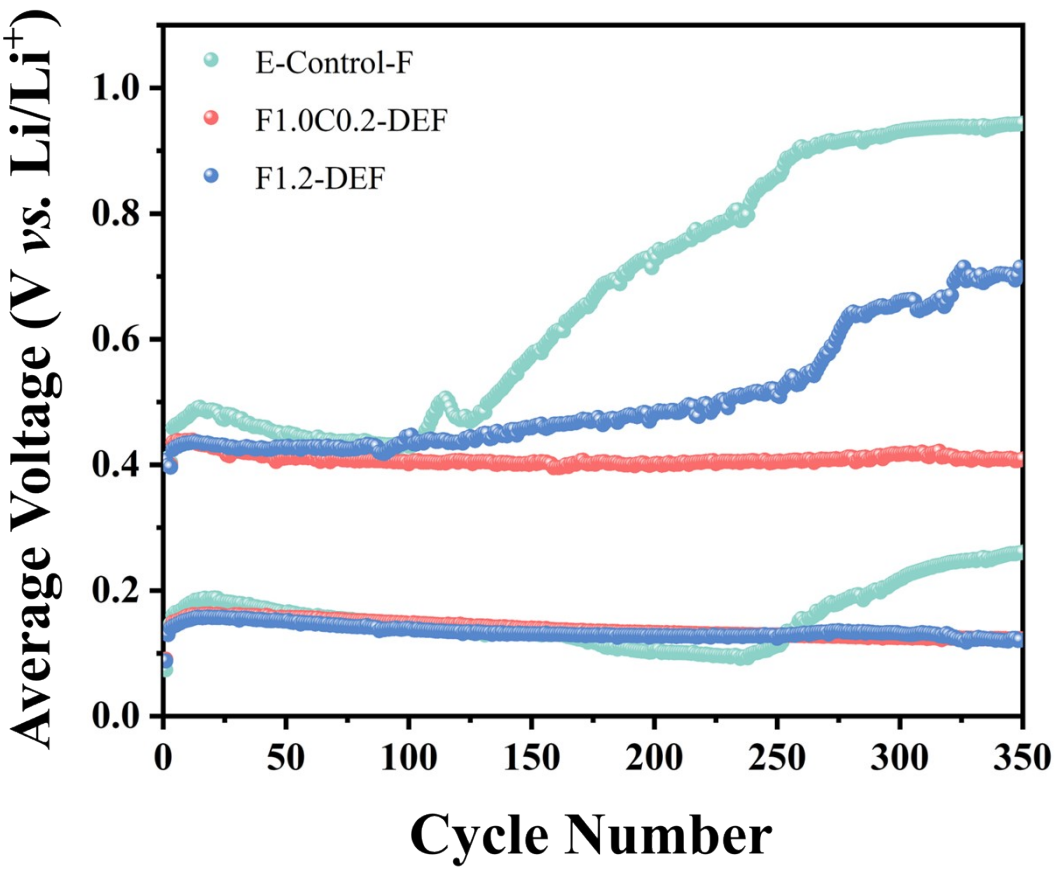

Fig. S10. Average charge/discharge potentials of Li||Si/C batteries cycled at 0.33C under 25 °C.

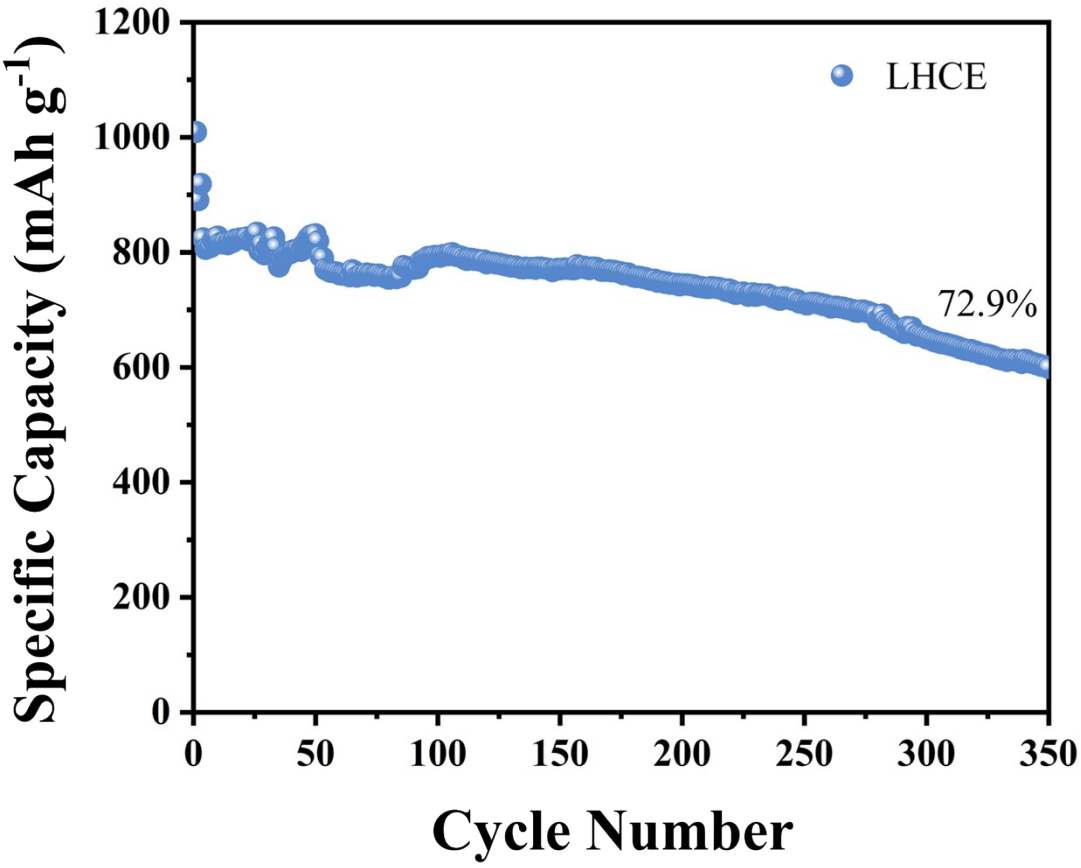

Fig. S11. Cycling performance of Li||Si/C batteries with the conventional localized high-concentration electrolyte (LHCE, 1.0 M LiFSI in DME/TTE (1:3.5, *v/v*)) at 0.33C under 25 °C (0.001 – 1.6 V). The cell was initially activated with one cycle at 0.05C (1C = 1100 mA g^{-1}), followed by two cycles at 0.1C.

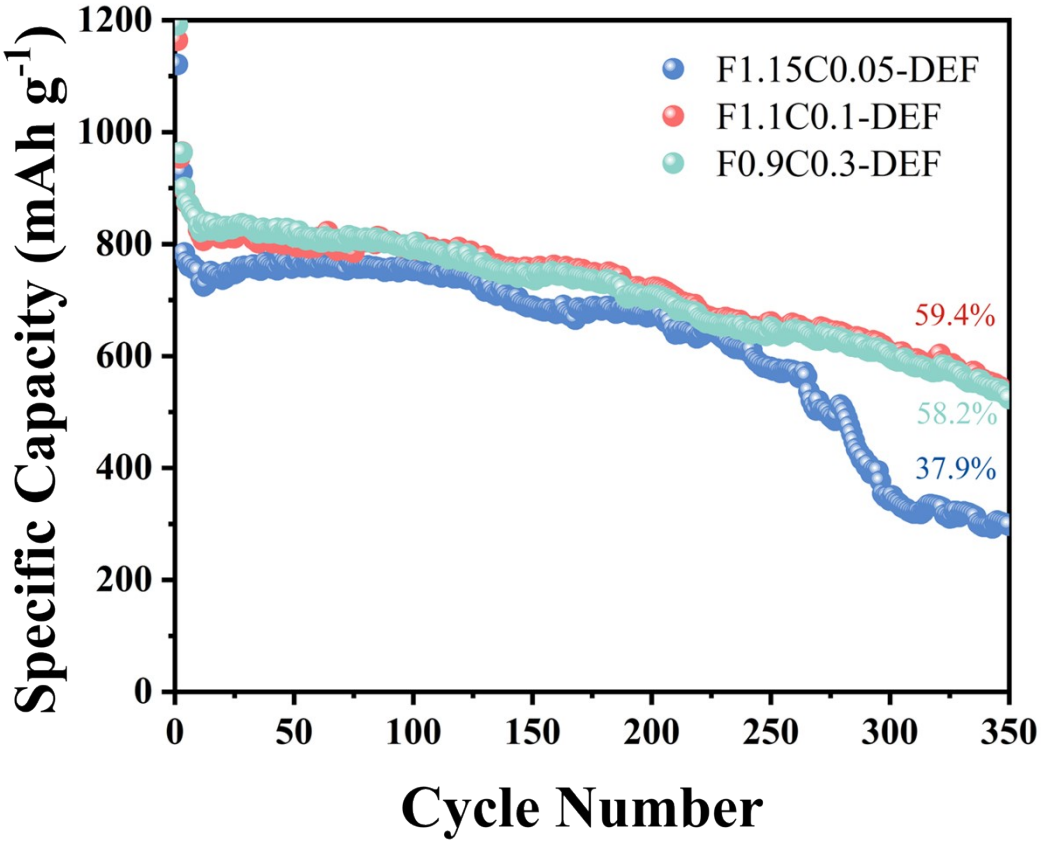

Fig. S12. Cycling performance of Li||Si/C batteries with F1.15C0.05-DEF, F1.1C0.1-DEF, and F0.9C0.3-DEF electrolytes at 0.33C under 25 °C (0.001 – 1.6 V). All cells were initially activated with one cycle at 0.05C (1C = 1100 mA g^{-1}), followed by two cycles at 0.1C.

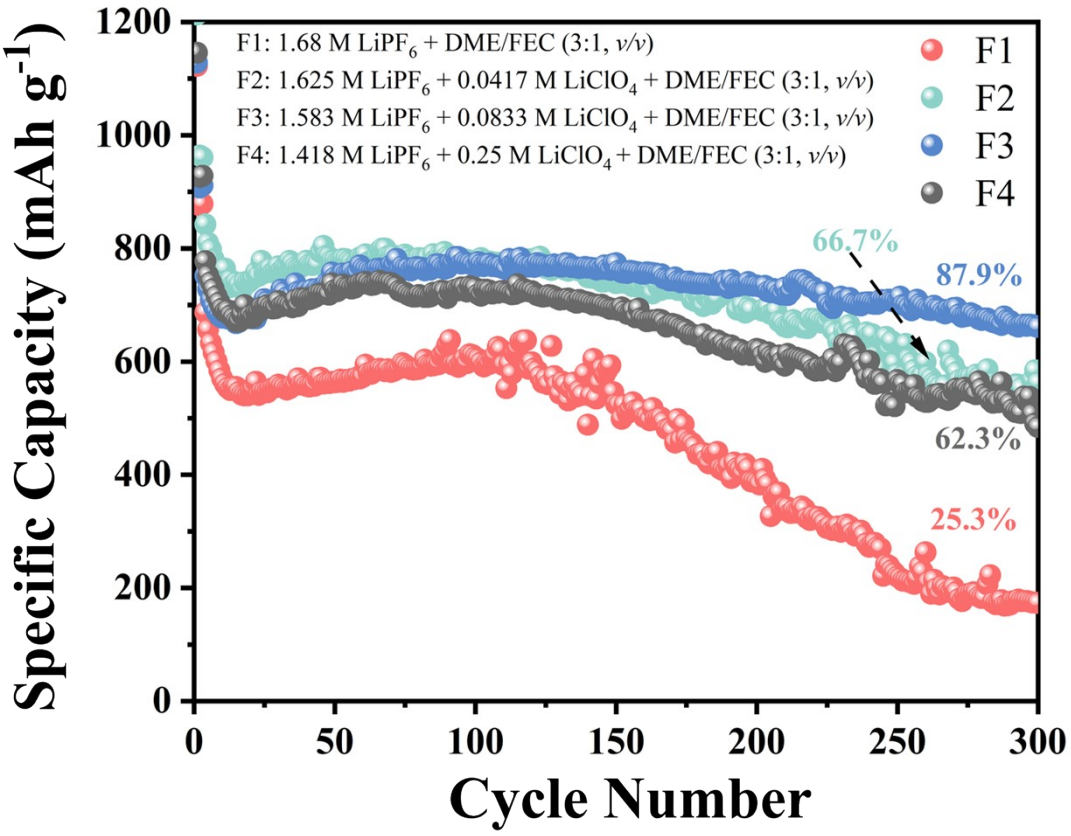

Fig. S13. Cycling performance of Li||Si/C batteries with F1, F2, F3, and F4 electrolytes at 0.33C under 25 °C (0.001 – 1.6 V). All cells were initially activated with one cycle at 0.05C (1C = 1100 mA g^{-1}), followed by two cycles at 0.1C.

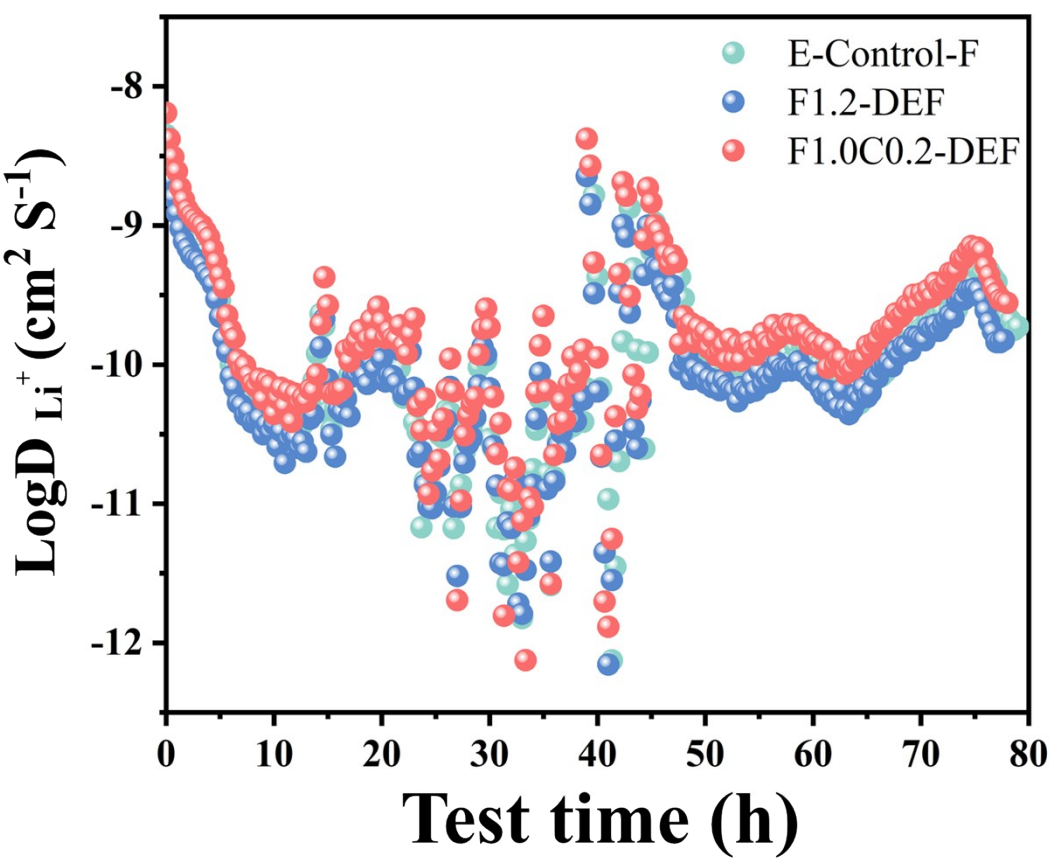

Fig. S14. Lithium-ion diffusion coefficients of the Si/C electrodes at the 10th cycle in E-Control-F, F1.2-DEF, and F1.0C0.2-DEF electrolyte (after 3 formation cycles at 0.1C), as calculated from GITT voltage profiles in Fig. S15.

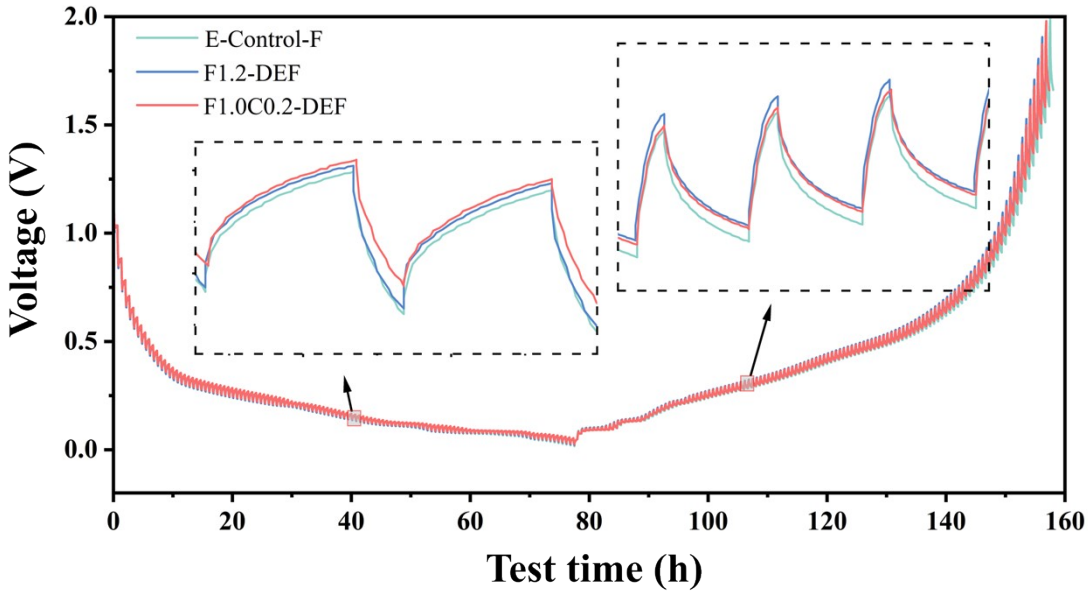

Fig. S15. GITT profiles of Li||Si/C cells with different electrolytes to evaluate lithium diffusion kinetics.

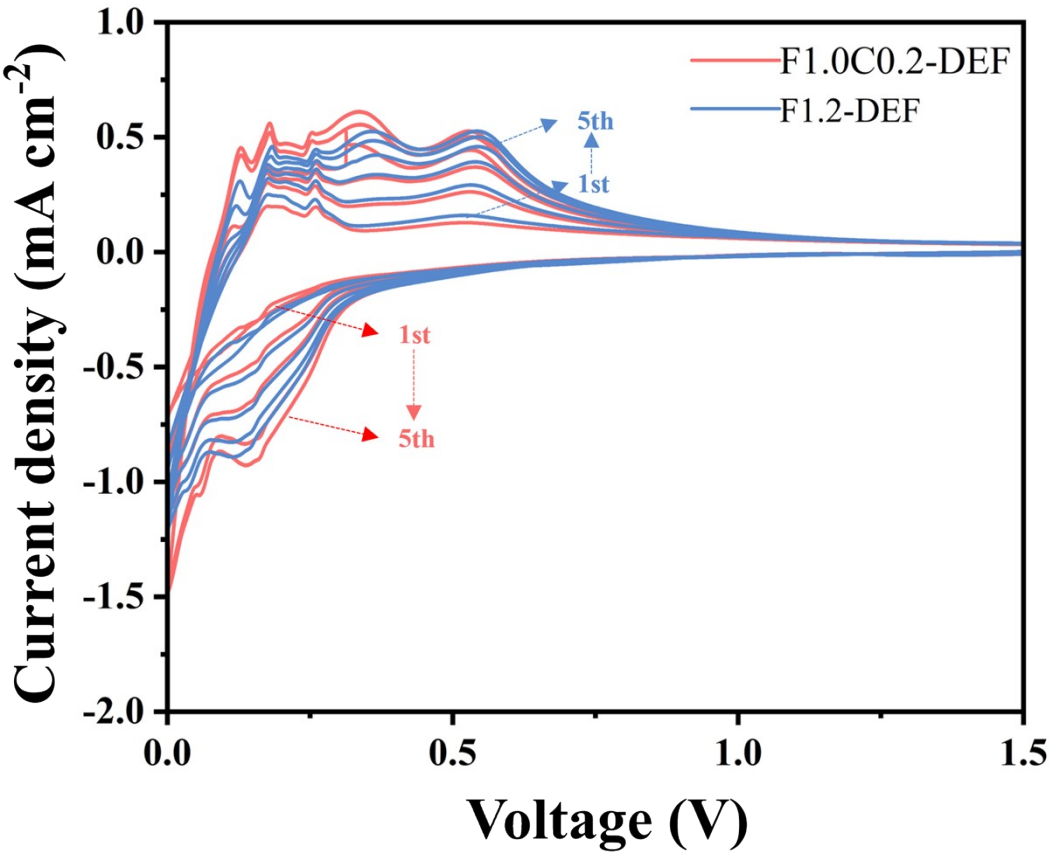

Fig. S16. CV plots of Li||Si/C cells in F1.0C0.2-DEF and F1.2-DEF at a scan rate of 0.05 mV s^{-1} (0.001 – 1.6 V).

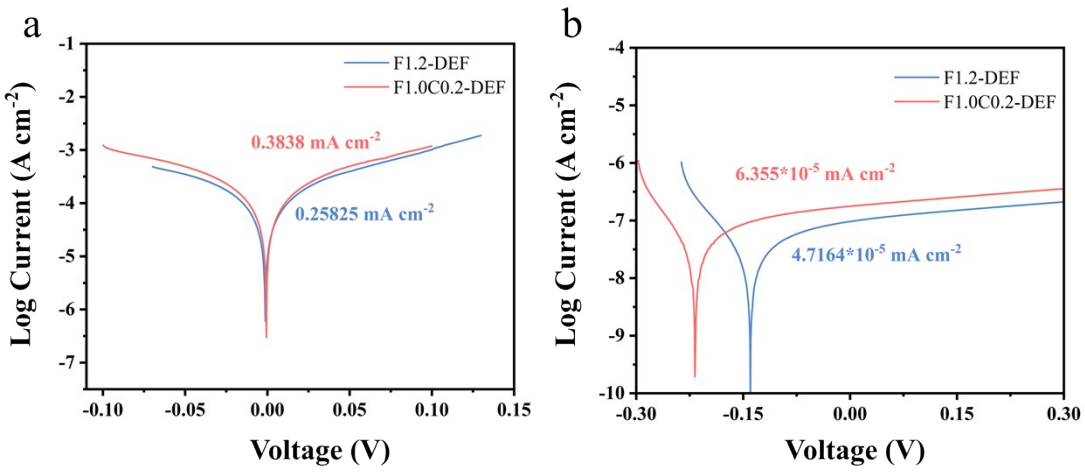

Fig. S17. Tafel polarization measurements of Li^+ kinetics in (a) Li||Li and (b) Si/C||Si/C symmetric cells using F1.2-DEF and F1.0C0.2-DEF at 25 °C (Scan rate: 1 mV s^{-1}).

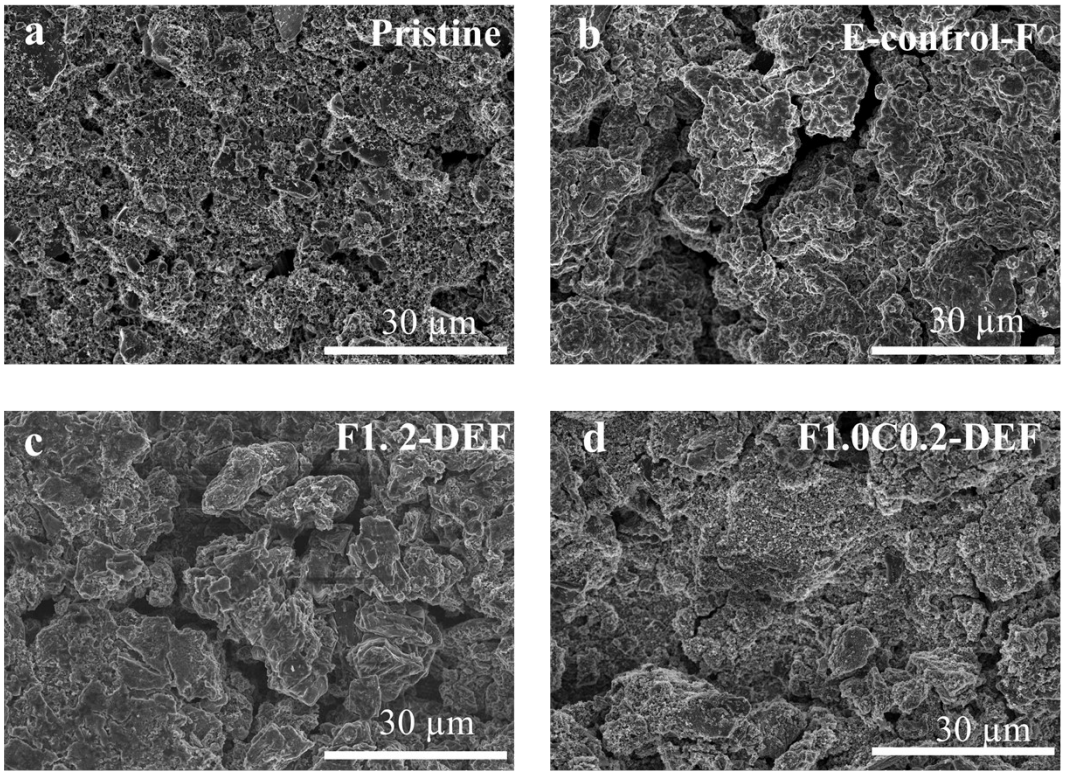

Fig. S18. SEM images of (a) pristine Si/C anodes and (b-d) cycled Si/C anodes after 100 times in (b) E-Control-F, (c) F1.2-DEF, and (d) F1.0C0.2-DEF.

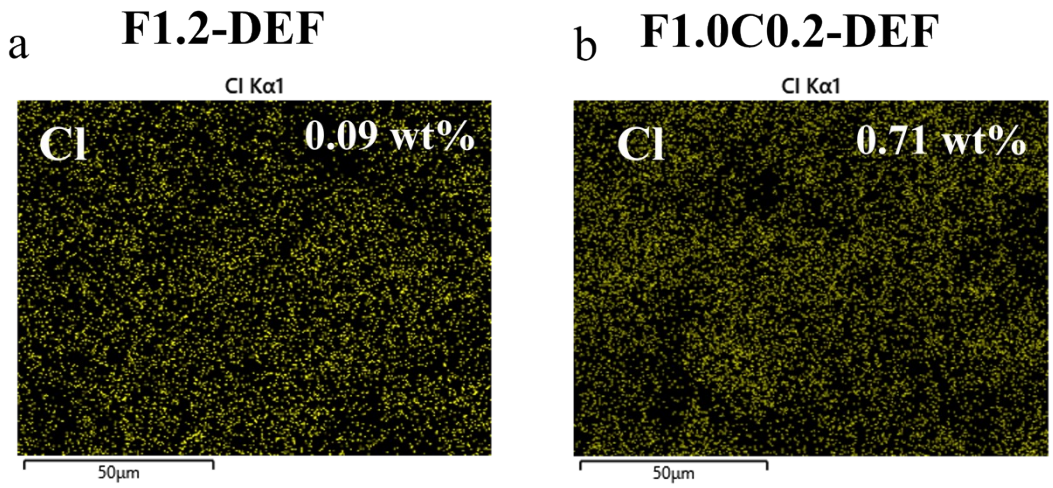

Fig. S19. EDS analysis of chlorine element distribution on cycled Si/C electrodes. (a) F1.2-DEF and (b) F1.0C0.2-DEF electrolytes after 100 cycles.

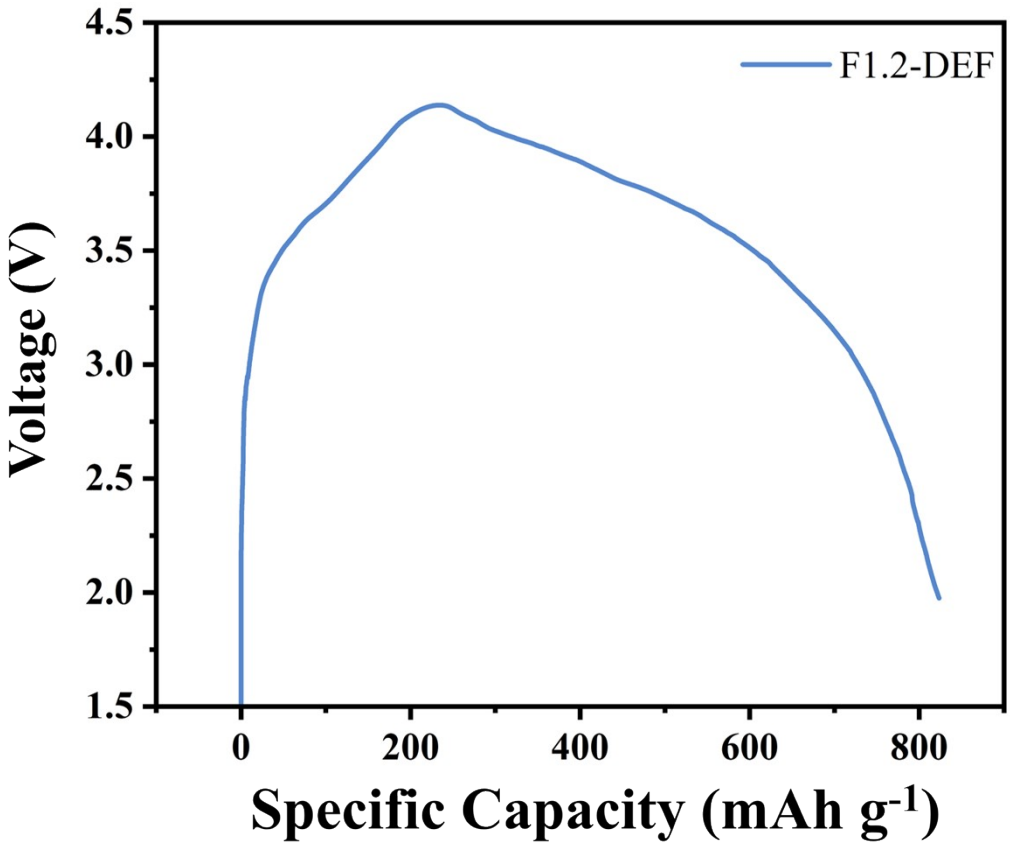

Fig. S20. Charge/discharge profile of Si/C||NCM811 cells in F1.2-DEF. The system shows charge failure at 4.2 V.

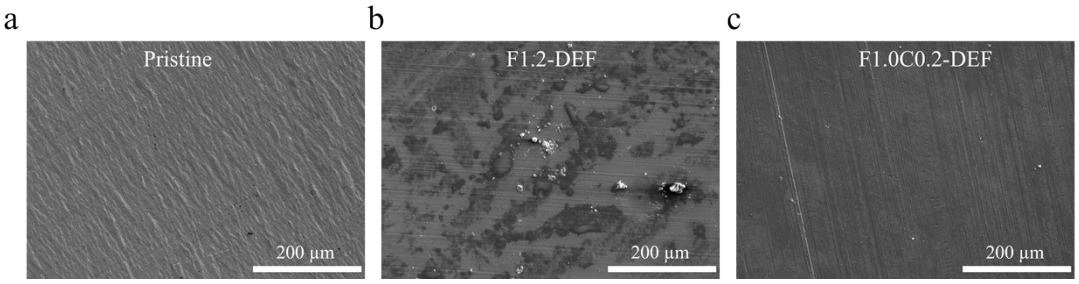

Fig. S21. Morphology of aluminum current collectors after electrochemical cycling. SEM images of (a) pristine Al foil (uncycled), and Al foils after 10 cycles in Si/C||NCM811 full cells (2.5 - 4.4 V) using (b) F1.2-DEF and (c) F1.0C0.2-DEF electrolytes.

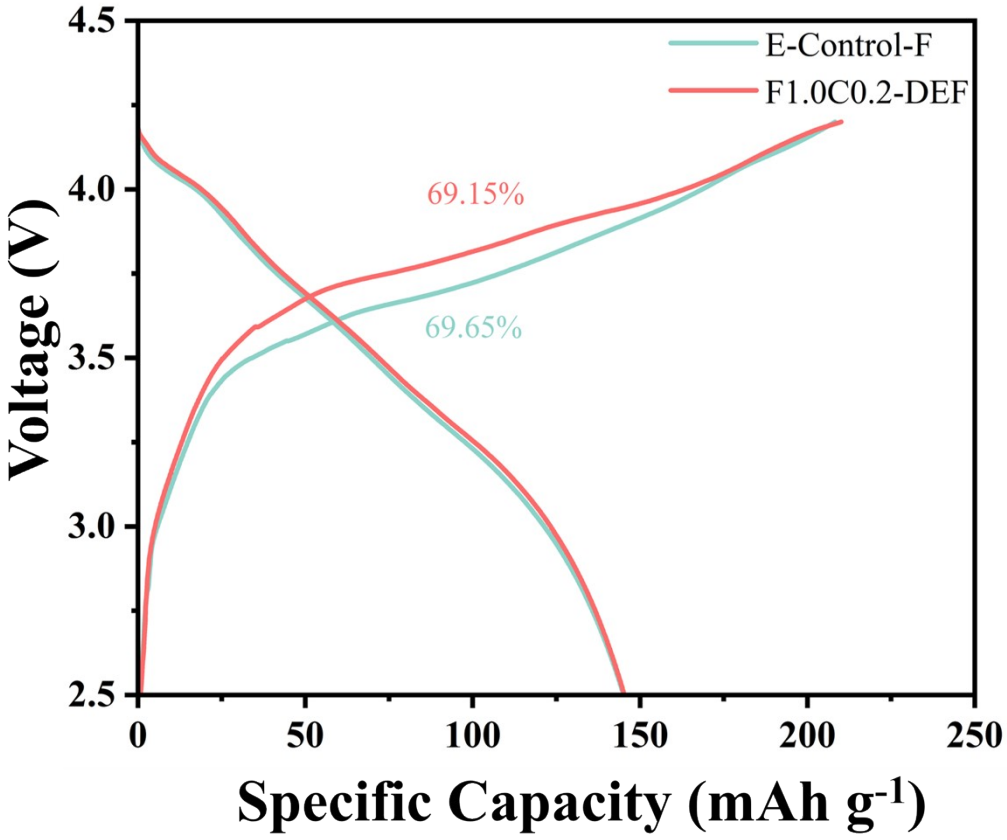

Fig. S22. The initial charge/discharge curves of Si/C||NCM811cells at 0.1 C. Substantial Li^+ consumption occurs during the initial cycle in both E-Control-F and F1.0C0.2-DEF electrolytes.

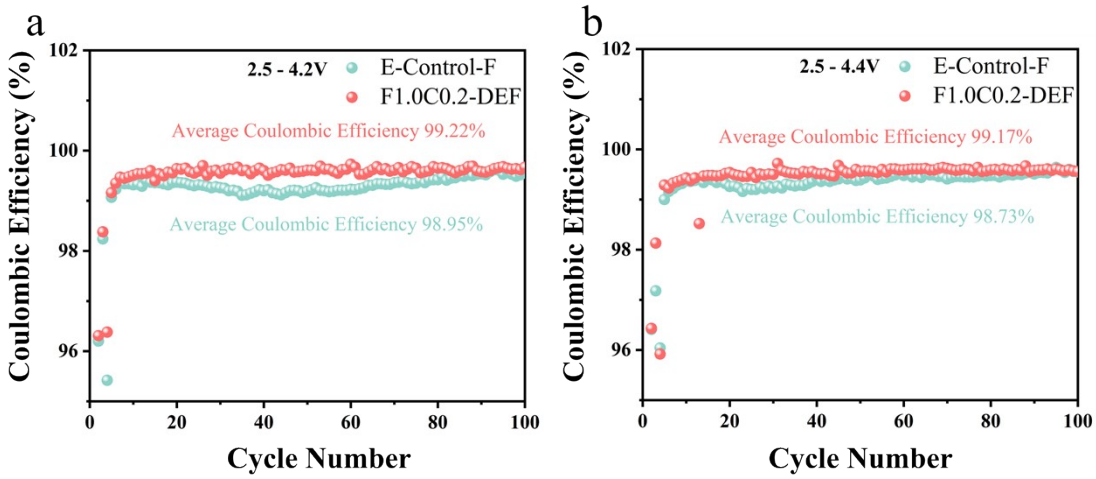

Fig. S23. Average Coulombic efficiency (Avg. CE) of Si/C||NCM811 full cells over the first 100 cycles. (a) Avg. CE at a charge cutoff voltage of 4.2 V. (b) Avg. CE at a charge cutoff voltage of 4.4 V.

Table S1. Cost Comparison Between F1.0C0.2-DEF and Silicon-Compatible Localized High-Concentration Electrolyte (Formulation 2: 1 M LiFSI + DME/1,1,2,2-Tetrafluoroethyl-2,2,3,3-tetrafluoropropyl ether (TTE) (1:3.5, *v/v)*).[1] Price data were obtained from Sigma-Aldrich (Merck Life Science) with prices current as of 4 July 2025. All chemicals were of battery grade purity (≥ 99.9%). The total electrolyte cost was calculated from individual component costs normalized to 1L solution volume at standard concentration (Lithium Salt Volume Excluded).

Component	**Price (RMB)**	**F1.0C0.2-DEF**	**Cost (RMB)**	**Formulation 2**	**Cost (RMB)**
LiFSI	95229.80 / kg	187 g	17807.97	187g	17807.97
$LiClO_4$	32676.76 / kg	21.28 g	695.36	-	-
DME	2464.98 / L	500 mL	1232.49	222.2 mL	547.22
EC	18304.44 / kg	498.75 g	9129.34	-	-
FEC	30663.57 / kg	218.1 g	6687.72	-	-
TTE	23092.80 / kg	-	-	1192.32 g	27534.01
Total	-	-	35552.88	-	45889.20

Table S2. Electrolyte formulations in this study.

Electrolyte code	Electrolyte formulation
E-Control-F	1.0 M $LiPF_6$ in EC/EMC (ethyl methyl carbonate)/DMC (dimethyl carbonates) (1:1:1, *v/v/v*) + 5*wt*.% FEC
F1.2-DEF	1.2 M LiFSI in DME/EC/FEC (10:7:3, *v/v/v*).
F1.15C0.05-DEF	1.15 M LiFSI + 0.05 M $LiClO_4$ in DME/EC/FEC (10:7:3, *v/v/v*)
F1.1C0.1-DEF	1.1 M LiFSI + 0.1 M $LiClO_4$ in DME/EC/FEC (10:7:3, *v/v/v*)
F1.0C0.2-DEF	1.0 M LiFSI + 0.2 M $LiClO_4$ in DME/EC/FEC (10:7:3, *v/v/v*)
F0.9C0.3-DEF	0.9 M LiFSI + 0.3 M $LiClO_4$ in DME/EC/FEC (10:7:3, *v/v/v*)
F1	1.68 M $LiPF_6$ in DME/FEC (3:1, *v/v*)
F2	1.625 M $LiPF_6$ + 0.0417 M $LiClO_4$ in DME/FEC (3:1, *v/v*)
F3	1.583 M $LiPF_6$ + 0.0833 M $LiClO_4$ in DME/FEC (3:1, *v/v*)
F4	1.418 M $LiPF_6$ + 0.25 M $LiClO_4$ in DME/FEC (3:1, *v/v*)
LHCE	1 M LiFSI + DME/TTE (1:3.5, *v/v*)

Table S3. Calculated HOMO and LUMO energy levels of solvation clusters with FSI^- and ClO_4^- anions. The DFT-calculated electronic properties include complexes with DME, EC, and FEC solvents, elucidating the synergistic effect of dual anions on reduction and oxidation stability.

System	LUMO (eV)	HOMO (eV)
ClO_4^-	4.41	-3.06
FSI^-	3.10	-4.36
Li^+-ClO_4^--DME	-1.24	-6.64
Li^+-FSI^--DME	-1.15	-8.19
$2Li^+$-FSI^--ClO_4^--DME	-3.19	-7.36
Li^+-ClO_4^--EC	-1.78	-6.59
Li^+-FSI^--EC	-1.66	-8.03
$2Li^+$-FSI^--ClO_4^--EC	-3.41	-7.35
Li^+-ClO_4^--FEC	-2.03	-6.68
Li^+-FSI^--FEC	-1.90	-8.14
$2Li^+$-FSI^--ClO_4^--FEC	-3.35	-7.56

Table S4. Performance summary of electrolyte research on Si-based anode in recent years.

Anode	**Capacity retention**	**Rate**	**Lithium salt concentration and type**	reference
Si/C	85.2% (350 cycles)	0.33C 1 C = 1100 mA g^{-1}	1.0 M LiFSI + 0.2 M $LiClO_4$	This work
Si/C	73.4% (300 cycles)	0.33 C 1 C = 1000 mA g^{-1}	~3.95 M LiFSI	2
Si/C	84.6% (50 cycles)	0.33 C 1 C = 1000 mA g^{-1}	4.5 M LiFSI	3
Si/C	85.4% (400 cycles)	0.5 C 1 C = 950 mA g^{-1}	~4.3 M LiFSI	4
Si/C	61.6% (250 cycles)	0.5 C 1 C = 700 mA g^{-1}	1.0 M $LiPF_6$	5
SiO_x/C	83% (80 cycles)	0.5 C 1 C = 650 mA g^{-1}	0.8 M $LiPF_6$	6
SiO_x/C	78.5% (500 cycles)	0.5 C 1 C = 800 mA g^{-1}	~2.0 M LiFSI + ~0.2 M $LiPF_6$	7
Si/C	71.2% (300 cycles)	0.5 C 1 C = 600 mA g^{-1}	1.0 M $LiPF_6$	8
SiO_x/C	79.3% (200 cycles)	0.5 C 1 C = 1000 mA g^{-1}	1.0 M $LiPF_6$	9
SiO_x/C	48% (150 cycles)	0.5C 1 C = 800 mA g^{-1}	1.0 M $LiPF_6$	10
SiO_x/C	85.4% (100 cycles)	0.1C 1 C = 450 mA g^{-1}	1.0 M $LiPF_6$	11
Si/C	72% (100 cycles)	0.1C 1 C = 623 mA g^{-1}	1.0 M LiTFSI	12
Si/C	98.11% (50 cycles)	0.2C 1 C = 550 mA g^{-1}	1.0 M $LiPF_6$	13
SiO_x/C	97.02% (100 cycles)	0.5C 1 C = 1000 mA g^{-1}	1.2 M $LiPF_6$	14
Si/C	70% (50 cycles)	0.5C 1 C = 700 mA g^{-1}	1.0 M $LiPF_6$	15
SiO_x/C	71% (400 cycles)	0.2C 1 C = 450 mA g^{-1}	1.0 M $LiPF_6$	16
Si/C	95.3% (100 cycles)	0.5C 1 C = 450 mA g^{-1}	1.15 M $LiPF_6$	17

Table S5. Fitted impedance parameters of Li‖Si/C cells with three different electrolytes.

	E-Control-F		**F1.2-DEF**		**F1.0C0.2-DEF**	
	R_{SEI} (Ω)	**R_{ct} (Ω)**	**R_{SEI} (Ω)**	**R_{ct} (Ω)**	**R_{SEI} (Ω)**	**R_{ct} (Ω)**
10th	5.12	8.07	1.73	15.01	1.17	12.06
250th	65.29	24.57	44.85	28.18	11.47	15.34

References

1 G. Yang, S. Frisco, R. Tao, N. Philip, T. H. Bennett, C. Stetson, J.-G. Zhang, S.-D. Han, G. Teeter, S. P. Harvey, Y. Zhang, G. M. Veith and J. Nanda, *ACS Energy Lett.*, 2021, **6**, 1684–1693.

2 H. Jia, L. Zou, P. Gao, X. Cao, W. Zhao, Y. He, M. H. Engelhard, S. D. Burton, H. Wang, X. Ren, Q. Li, R. Yi, X. Zhang, C. Wang, Z. Xu, X. Li, J. Zhang and W. Xu, *Adv. Energy Mater.*, 2019, **9**, 1900784.

3 S. Chae, W.-J. Kwak, K. S. Han, S. Li, M. H. Engelhard, J. Hu, C. Wang, X. Li and J.-G. Zhang, *ACS Energy Lett.*, 2021, **6**, 387–394, .

4 Z. Ma, D. Ruan, D. Wang, Z. Lu, Z. He, J. Guo, J. Fan, J. Jiang, Z. Wang, X. Luo, J. Ma, Z. Zhang, Y. You, S. Jiao, R. Cao and X. Ren, *Angew. Chem. Int. Ed.*, 2024, **64**, e202414859.

5 Z. Hu, L. Zhao, T. Jiang, J. Liu, A. Rashid, P. Sun, G. Wang, C. Yan and L. Zhang, *Adv. Funct. Mater.*, 2019, **29**, 1906548.

6 S.-J. Tan, Y.-F. Tian, Y. Zhao, X.-X. Feng, J. Zhang, C.-H. Zhang, M. Fan, J.-C. Guo, Y.-X. Yin, F. Wang, S. Xin and Y.-G. Guo, J. Am. Chem. Soc., 2022, 144, 18240–18245.

7 G. Liu, M. Xia, J. Gao, Y. Cheng, M. Wang, W. Hong, Y. Yang and J. Zheng, *ACS Appl. Mater. Interfaces*, 2023, **15**, 3586–3598.

8 Z. Wen, F. Wu, L. Li, N. Chen, G. Luo, J. Du, L. Zhao, Y. Ma, Y. Li and R. Chen, *ACS Appl. Mater. Interfaces*, 2022, **14**, 38807–38814.

9 G. Liu, J. Gao, M. Xia, Y. Cheng, M. Wang, W. Hong, Y. Yang and J. Zheng, *ACS Appl. Mater. Interfaces*, 2022, **14**, 38281–38290.

10 G. Liu, T. Jiao, Y. Cheng, K. Zhou, Y. Zou, M. Wang, Y. Yang and J. Zheng, *ACS Appl. Energy Mater.*, 2021, **4**, 10323–10332.

11 G. Xu, X. Wang, J. Li, X. Shangguan, S. Huang, D. Lu, B. Chen, J. Ma, S. Dong, X. Zhou, Q. Kong and G. Cui, *Chem. Mater.*, 2018, **30**, 8291–8302.

12 L. Gehrlein, C. Leibing, K. Pfeifer, F. Jeschull, A. Balducci and J. Maibach, *Electrochim. Acta*, 2022, **424**, 140642.

13 H. Lu, F. Zeng, Y. Ma, M. Liu, B. Zhou, Z. Zhang, H. Liu and Y. Yuan, *Mater. Today Commun.*, 2023, **35**, 105619.

14 R. Wang, J. Cao, C. Xu, N. Wu, S. Zhang and M. Wu, *RSC Adv.*, 2023, **13**, 13365–13373.

15 H. Liu, A. J. Naylor, A. S. Menon, W. R. Brant, K. Edström and R. Younesi, *Adv. Mater. Interfaces*, 2020, **7**, 2000277.

16 W. Cheng, N. Li, J. Liu, S. Ma and X. Gao, *ACS Appl. Mater. Interfaces*, 2023, **15**, 51025–51035.

17 H. Kang, H. Kim, C. Yeom and M. J. Park, *ACS Appl. Energy Mater.*, 2022, **5**, 4673–4683.